



30th Eurosensors Conference, EUROSENSORS 2016

Bandwidth Optimisation and Frequency Tuning of Plasmonic Functionalised Metasurfaces for Optical Sensing of Chemical and Biological Substances

M. Janneh, A. De Marcellis*, E. Palange

University of L'Aquila, Department of Industrial and Information Engineering and Economics, Via G. Gronchi 18, L'Aquila 67100, Italy

Abstract

This paper reports on a method to optimise the sensitivity of plasmonic sensors based on functionalised metasurfaces of 2D-array of Al NanoAntennas (NA) deposited on a SiO₂ substrate operating in the visible region of the electromagnetic spectrum. Moreover, we analysed the characteristics of a double layer metasurface configuration where two different NA 2D-arrays are separated by a dielectric spacer. The optical properties of both the metasurface configurations have been studied analysing how their maximum transmittance and Full-Width-at-Half-Maximum (FWHM) of the transmission curve are related to the variations of the NA geometrical parameters and dielectric spacer thickness. The tailoring of the FWHM is particular important for improving the plasmonic sensors sensitivity in probing the presence of chemical/biological substances adsorbed on the NA surface when their absorption curve is superimposed with the metasurface transmission curve. In particular, better is this superposition better will be the plasmonic sensor sensitivity in probing variations of small concentrations of the adsorbed substances. The simulation results of the optical response of the designed plasmonic sensors suggest a methodology in choosing the NA parameters able to modify the bandwidth of the metasurface transmittance so fitting the absorption curve of chemical/biological substances adsorbed on them. As a case-example, we simulated the response of a plasmonic sensor on which has been deposited a 3nm-thick layer of Rhodamine-6G (R6G) proving that is possible to increase the sensor detection sensitivity of about two orders of magnitude in the measurement of the R6G absorbance. Furthermore we proved the capability of the double layer plasmonic sensors to tune the transmission curve peak wavelength without changing the main optical characteristics.

© 2016 The Authors. Published by Elsevier Ltd. This is an open access article under the CC BY-NC-ND license (<http://creativecommons.org/licenses/by-nc-nd/4.0/>).

Peer-review under responsibility of the organizing committee of the 30th Eurosensors Conference

Keywords: Functionalised Metasurfaces; Plasmonic Sensors; SEIRA.

* Corresponding author. Tel.: +39 0862 434424; fax: +39 0862 434403.
E-mail address: andrea.demarcellis@univaq.it

1. Introduction

In chemical, bioscience and bioengineering applications, optical methods are widely used for the characterisation, identification and modification of substances, cells and organelles by measuring light absorption, scattering and emission [1,2]. Optical sensors provide the advantages to have high sensitivities with short response times, to be unaffected from electromagnetic interferences and to perform non-destructive measurements, also far from the sample under analysis. In particular, optical sensors make use of different analytical transduction techniques such as fluorescence, chemiluminescence, dynamic light scattering, ellipsometry, surface enhanced Raman scattering, Surface Enhanced Infrared Absorption (SEIRA) and surface plasmon resonances [3-10]. The implementation of the latter three approaches need the use of metal nanoparticles or nanostructures arranged in 2D-array configurations (i.e., functionalised metasurfaces) to provide local strong enhancement of the electromagnetic field so to improve the light emitted, reflected and/or transmitted by the substance adsorbed on them [9,11]. In particular, SEIRA technique makes use of metasurfaces composed by 2D-arrays of metal NAs with optical properties related to the light transmission and reflection responses as a function of the wavelength. In this sense, the NA size and 2D-array periodicity can be varied to control the peak wavelength of the transmission or reflection curves. By using a cross-shaped NA as the constitutive element of a 2D-array metasurface, it has been demonstrated that the SEIRA gain (i.e., a signature of the optical sensor sensitivity to the presence of a substance adsorbed on it) can be increased of orders of magnitude by acting on the length and width of the cross arms as well as on the NA thickness [12]. SEIRA technique is based on the spectral superposition of the reflection/transmission curve of the metasurface with the absorption curve of the adsorbed substance. Better is this overlapping better will be the optical sensor detection sensitivity. This paper addresses the problem to find a methodology that acting on the NA size is able to vary the bandwidth of the metasurface reflection/transmission response so tailoring it respect to the absorption curve of the substance under analysis. By performing numerical simulations, we firstly evaluated the optical transmittance of a metasurface composed of a 2D-array of Al NA deposited on SiO₂. In particular, we evaluated the FWHM of the transmittance and its maximum value at a fixed wavelength in the visible region of the electromagnetic spectrum. These results have been used to study the increases of the sensitivity of the metasurface in detecting the presence of a 3nm-thick layer of R6G deposited on it. Like other dyes with absorption bands ranging from 400 to 700nm, R6G is a chromophore to detect biological species [13]. In this regards, we also studied wavelength tuning properties of double layer metasurface configurations where a dielectric spacer separates the two metasurfaces.

2. Results and discussion

The 2D-array unit cell (i.e., the Al NA) for the single layer metasurface configuration used for the simulations is reported in Figure 1 (on the right of panel (a)). The NA can be obtained by etching procedures starting from a $t=40\text{nm}$ thick homogeneous Al film deposited on a SiO₂ substrate. The NA is composed of a square frame with the external and inner sides equal to L_e and L_i , respectively. Inside the square frame is located a cylinder with a diameter d . The surface between the internal side of the frame and the cylinder is optically transparent since Al film is removed. The optical properties of the metasurface were obtained by using periodic boundary conditions along the x - and y -axes (i.e., the NA plane) and the scattering boundary conditions along the z -axis (i.e., the propagation direction of the light impinging on the metasurface). The incident electric field was set to $|\mathbf{E}_0|=1\text{V/m}$ with the linear polarization $\mathbf{E}_0 = \mathbf{E}_{0,x} + \mathbf{E}_{0,y}$. The typical metasurface optical transmission centred at $\lambda_p=530\text{nm}$ is shown in panel (b) of Figure 1. The left panel of Figure 2 reports the dependence of the metasurface transmittance and its FWHM on the variation of the NA area of the transparent region. From the achieved data, a decrease of the FWHM is obtained at the expenses of a reduction of the effective metasurface transmittance confirming the general behaviour valid, for example, for the optical bandpass filters using interference effects. Once demonstrated the possibility to vary the FWHM of the metasurface transmission curve, a 3nm thick layer of R6G at 0.01 molar concentration in methanol was located on top of the single layer metasurface configuration. Under these conditions, simulations were performed to evaluate the SEIRA gain at $\lambda_p=530\text{nm}$ defined as the ratio between the difference of the metasurface transmittances in presence and absence of the R6G layer and the transmittance of the same R6G layer deposited on a SiO₂ substrate.

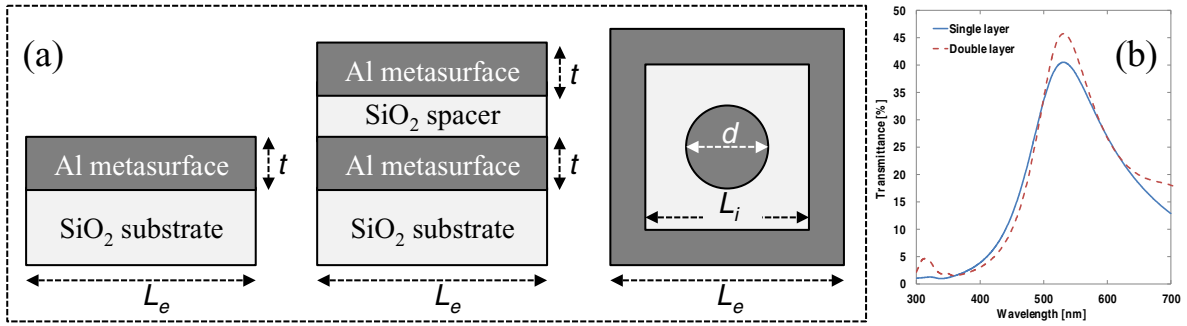


Fig. 1. Panel (a): on the left, the cross section of the single layer metasurface configuration with the Al NA forming the 2D-array having the geometrical structure shown on the right; on center, the cross section of the double layer metasurface configuration obtained by superposing on the previous configuration a thin SiO_2 spacer and a top layer formed by 2D-array of Al NA having the geometrical structure shown on the right without the internal cylinder; on the right, the plane view of the geometrical structure of the unit cell. Panel(b): the metasurface transmission responses centered at $\lambda_p=530\text{nm}$ for the single and double layer metasurface configurations.

The right panel of Figure 2 shows that the decrease of the metasurface FWHM increases the SEIRA gain up to 70 and this accounts for a better superimposition between the metasurface transmittance and the R6G absorption curves. Since chromophores have absorption peak wavelengths varying in the range from 400 to 800nm, the optimisation of metasurfaces allowing for the best achievable SEIRA gain must be each time redefined being their optical response depending on the NA size and 2D-array periodicity. The double layer metasurface configuration shown in panel (a) of Figure 1 allows for a continuous wavelength tuning maintaining fixed the NA geometry. This metasurface configuration has been obtained by locating on top of the metasurface single layer structure a SiO_2 spacer and a metasurface of NA with a geometrical structure that does not present the internal cylinder. On the left panel of Figure 3 are reported the variations of the transmission curve peak wavelength and of the corresponding value of the maximum transmittance as a function of the spacer thickness. The tuning of the peak wavelength is a linear function of the spacer thickness: a variation of this thickness of 80nm allows covering the range from 480nm (blue) to 640nm (red). In the right panel of Figure 3 is reported the FWHM of the double layer metasurface transmission curve and the maximum transmittance as a function of the variation of the NA transparent area. A comparison with the results previously obtained for the single layer metasurface demonstrates that the achievable FWHM are smaller than those ones of Figure 2. As an example, for a value of the NA transparent area equal to 16000nm^2 the corresponding FWHM is equal to about 280nm and 155nm for the single and double layer metasurface configurations, respectively (i.e., a reduction of 56%). Note that, in this case, the corresponding maximum transmittances decrease from 66% to 34%. Finally, we have verified that for the same value of the FWHM, the SEIRA gain is always the same for both the metasurface configurations.

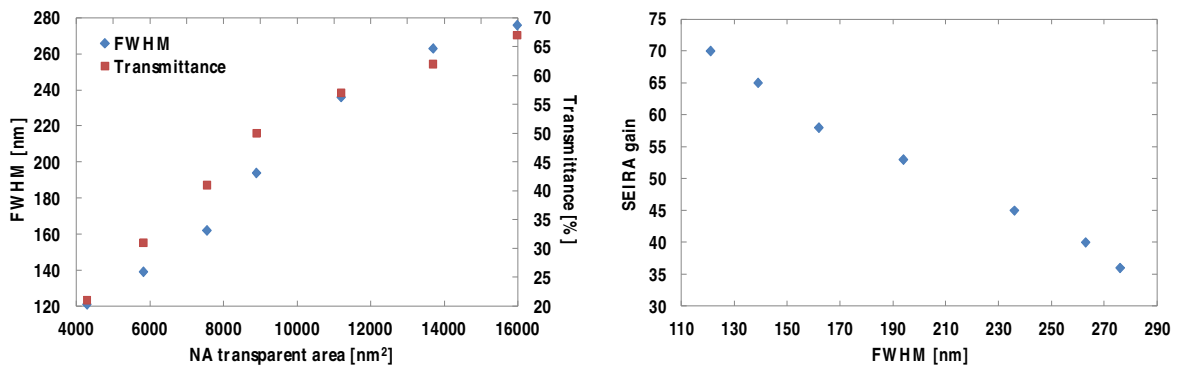


Fig. 2. Single layer metasurface configuration: transmission curve FWHM and maximum transmittance at $\lambda_p=530\text{nm}$ as a function of the NA transparent area (left); SEIRA gain as a function of the wavelength in presence of a 3nm thick R6G layer on top of the metasurface (right).

3. Conclusions

In this paper we reported on the optical characteristics of plasmonics sensors based on functionalised metasurfaces of 2D-array of Al NA deposited on a SiO_2 substrate in a single and double layer configurations operating in the visible region of the electromagnetic spectrum. By performing numerical simulations for both the configurations, we studied the dependence on the NA size of the metasurface transmission curve FWHM and of the corresponding maximum transmittance. This allowed to optimise the SEIRA gain in detecting substances adsorbed onto the metasurface. In the case of the double layer metasurface configuration, we have demonstrated that the peak wavelength of the transmission curve can be continuously varied by acting on the dielectric spacer that separates the two metasurface layers with advantages to further decrease the resulting FWHM.

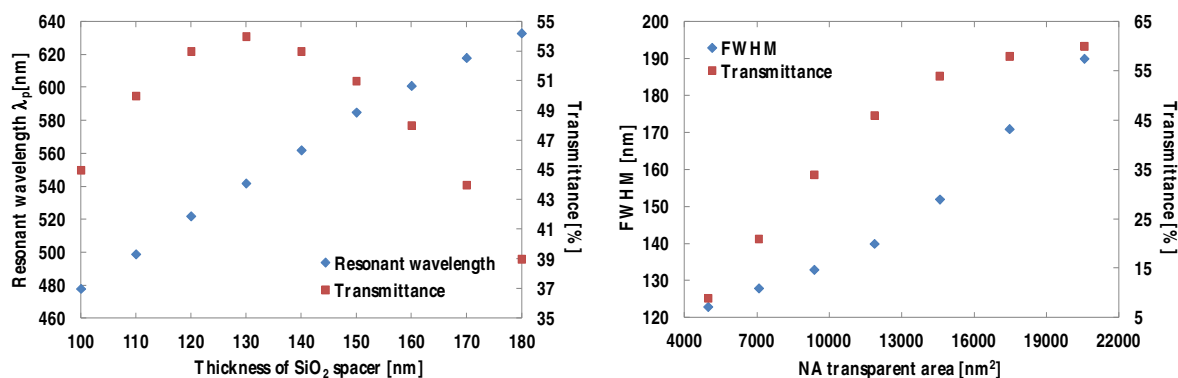


Fig. 3. Double layer metasurface configuration: the tuning of the transmittance peak wavelength as a function the spacer thickness (left); FWHM and transmittance versus the NA transparent area at $\lambda_p=530\text{nm}$ (right).

References

- [1] C. Feng, S. Dai, L. Wang, Optical aptasensors for quantitative detection of small biomolecules: A review, *Biosensors and Bioelectronics* 59 (2014) 64-74.
- [2] M.T. Cone, J.D. Mason, E. Figueroa, B.H. Hokr, J.N. Bixler, C.C. Castellanos, G.D. Noojin, J.C. Wagle, B.A. Rockwell, V.V. Yakovlev, E.S. Fry, Measuring the absorption coefficient of biological materials using integrating cavity ring-down spectroscopy, *Optica* 2 (2015) 162-168.
- [3] S. Lane, P. West, A. François, A. Meldrum, Protein biosensing with fluorescent microcapillaries, *Optics Express* 23 (2015) 2577-2590.
- [4] B. Fu, J. Cao, W. Jiang, L. Wang, A novel enzyme-free and label-free fluorescence aptasensor for amplified detection of adenosine, *Biosensors and Bioelectronics* 44 (2013) 52-56.
- [5] B.C. Galarreta, M. Tabatabaei, V. Guieu, E. Peyrin, F. Lagugné-Labarhet, Microfluidic channel with embedded SERS 2D platform for the aptamer detection of ochratoxin A, *Anal. Bioanal. Chem.* 405 (2013) 1613-1621.
- [6] Q. Wang, L. Yang, X. Yang, K. Wang, J. Liua, Use of mercaptophenylboronic acid functionalized gold nanoparticles in a sensitive and selective dynamic light scattering assay for glucose detection in serum, *Analyst* 138 (2013) 5146-5150.
- [7] Q. Wang, J. Huang, X. Yang, K. Wang, L. He, X. Li, C. Xue, Surface plasmon resonance detection of small molecule using split aptamer fragments, *Sensors and Actuators B: Chemical* 156 (2011) 893-898.
- [8] N. Michieli, B. Kalinic, C. Scian, T. Cesca, G. Mattei, Optimal geometric parameters of ordered arrays of nanoprisms for enhanced sensitivity in localized plasmon based sensors, *Biosensors and Bioelectronics* 65 (2015) 346-353.
- [9] R. Adato, H. Altug, In-situ ultra-sensitive infrared absorption spectroscopy of biomolecule interactions in real time with plasmonic nanoantennas, *Nat. Commun.* 4 (2013) 2154, 1-10.
- [10] S.H. Cao, Z.X. Zou, Y.H. Weng, W.P. Cai, Q. Liu, Y.Q. Li, Plasmon-mediated fluorescence with distance independence: From model to a biosensing application, *Biosensors and Bioelectronics* 58 (2014) 258-265.
- [11] J.E. Kim, J.H. Choib, M. Colasa, D.H. Kimb, H. Lee, Gold-based hybrid nanomaterials for biosensing and molecular diagnostic applications, *Biosensors and Bioelectronics* 80 (2016) 543-559.

- [12] A. De Marcellis, E. Palange, M. Janneh, C. Rizza, A. Ciattoni, S. Mengali, Design optimisation of plasmonic metasurfaces for mid-infrared high-sensitivity chemical sensing, *Plasmonics* (2016) DOI: 10.1007/s11468-016-0263-9, *in press*.
- [13] M.B. Gonçalves, J. Dreyer, P. Lupieri, C. Barrera-Patiño, E. Ippoliti, M.R. Webb, J.E. Corrie, P. Carloni, Structural prediction of a rhodamine-based biosensor and comparison with biophysical data, *Phys. Chem. Chem. Phys.* 15 (2013) 2177-2183.